Bioorganic Chemistry 87 (2019) 191–199

Contents lists available at ScienceDirect

Bioorganic Chemistry

journal homepage: www.elsevier.com/locate/bioorg

Pomalidomide hybrids act as proteolysis targeting chimeras: Synthesis, anticancer activity and B-Raf degradation

Hong Chen[1], Feihong Chen[1], Sinan Pei, Shaohua Gou*

Pharmaceutical Research Center and School of Chemistry and Chemical Engineering, Jiangsu Province Hi-Tech Key Laboratory for Biomedical Research, Southeast University, Nanjing 211189, PR China

ARTICLE INFO

Keywords:
Pomalidomide
Proteolysis targeting chimeras
B-Raf
Anticancer activity

ABSTRACT

As the first intracellular signaling molecule and the most frequently mutated oncogene, B-Raf represents an important target in cancer therapy. Here we report several pomalidomide hybrids acting as proteolysis targeting chimeras (PROTACs) for the degradation of B-Raf. Due to its high expression of B-Raf, MCF-7 cells are sensitive to these compounds. Among them, compound **2** can effectively kill cancer cells via inducing cells apoptosis. As a B-Raf degrader, compound **2** can accelerate the degradation of B-Raf by recruiting ubiquitin-proteasome system, and further affects the expression of Mcl-1, a downstream protein of B-Raf. The anticancer mechanism of compound **2** is quite different from its mother compound and cancer cells seem to be more sensitive to the degrader, hinting that degradation of B-Raf by PROTAC is a potential way for cancer treatment.

1. Introduction

Immunomodulatory drugs (IMiDs, Fig. 1) are a class of orally available anticancer agents derived from thalidomide, which eventually turned out to be responsible for infants with phocomelia when used as a sedative for pregnant women [1,2]. Despite the serious defect, thalidomide was serendipitously found to be potent in the treatment of multiple myeloma (MM) due to its immune-modulation, anti-angiogenic and anti-inflammatory effects [3,4]. Until 2010, Ito and co-workers successfully identified cereblon (CRBN) as the thalidomide-binding protein [5]. CRBN is a subunit of the cullin-4-containing E3 ubiquitin ligase complex CRL4, which can promote the neighboring protein to degrade via ubiquitination [6].

As the third generation IMiDs, pomalidomide approved by US FDA in 2013 for patients with MM who have received at least two prior therapies was more effective and less toxic than thalidomide and lenalidomide [7,8]. Like thalidomide, pomalidomide has the comparable affinity for CRBN [9]. However, the difference is that, the presence of the substituent at benzene provides the ability to mediate the interaction of CRBN with neosubstrates that are not typically targeted by CRL4 [6,10,11]. These findings opened a new field of selective ubiquitination and degradation of specific targets by regulating the interaction of CRBN-based E3 ubiquitin ligase with target protein.

Proteolysis targeting chimera (PROTAC) is a heterobifunctional molecule consisting of an E3 ligase-binding group and another ligand binging to the protein of interest (POI), which are conjugated via a linker [12,13]. A number of small molecular-based PROTACs using thalidomide derivative as the recruiter of E3 ubiquitin ligase had been developed [14–16]. As shown in Fig. 2, a conjugate (DAS-6-2-2-6-CRBN) of pomalidomide with dasatinib, a chemotherapy drug used to treat chronic myelogenous leukemia (CML) and acute lymphoblastic leukemia (ALL) via targeting oncogenic BCR-ABL, was designed by Crews and co-workers, the compound could effectively induce the degradation of BCR-ABL despite some loss in affinity for the target [17]. Another representative PROTAC, named as dBET1, synthesized by Bradner and co-workers could selectively mediate the degradation of BET protein through a CRBN-dependent manner [18]. Our group also developed a CK2 targeting PROTAC that could degrade CK2 protein in a dose and time dependent manner, and kept CK2 at a low basal level by recruiting ubiquitin-proteasome system [19]. As an emerging and promising approach for drug discovery, PROTAC strategy has been accelerated greatly in recent years, and it is worthy of exploring novel PROTACs that target different protein for degradation.

As the most frequently mutated oncogene in Raf kinase superfamily, B-Raf represents an important target in cancer, in part because of its overexpression in most of tumor cells, and also for it is the first intracellular signaling molecule that is responsible for cancer cell proliferation [20–22]. Rigosertib (RGS), a small molecule anticancer

* Corresponding author.
E-mail address: sgou@seu.edu.cn (S. Gou).
[1] These authors contributed equally.

https://doi.org/10.1016/j.bioorg.2019.03.035
Received 19 January 2019; Received in revised form 3 March 2019; Accepted 14 March 2019
Available online 19 March 2019

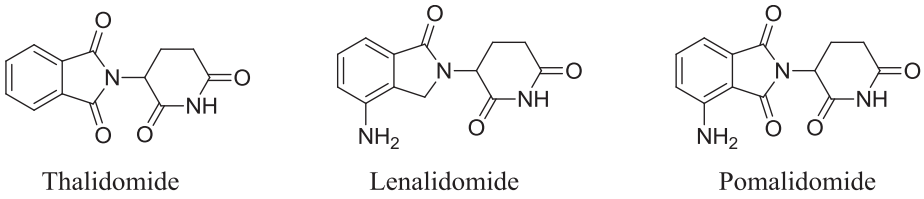

Fig. 1. Three immunomodulatory drugs: thalidomide, lenalidomide and pomalidomide.

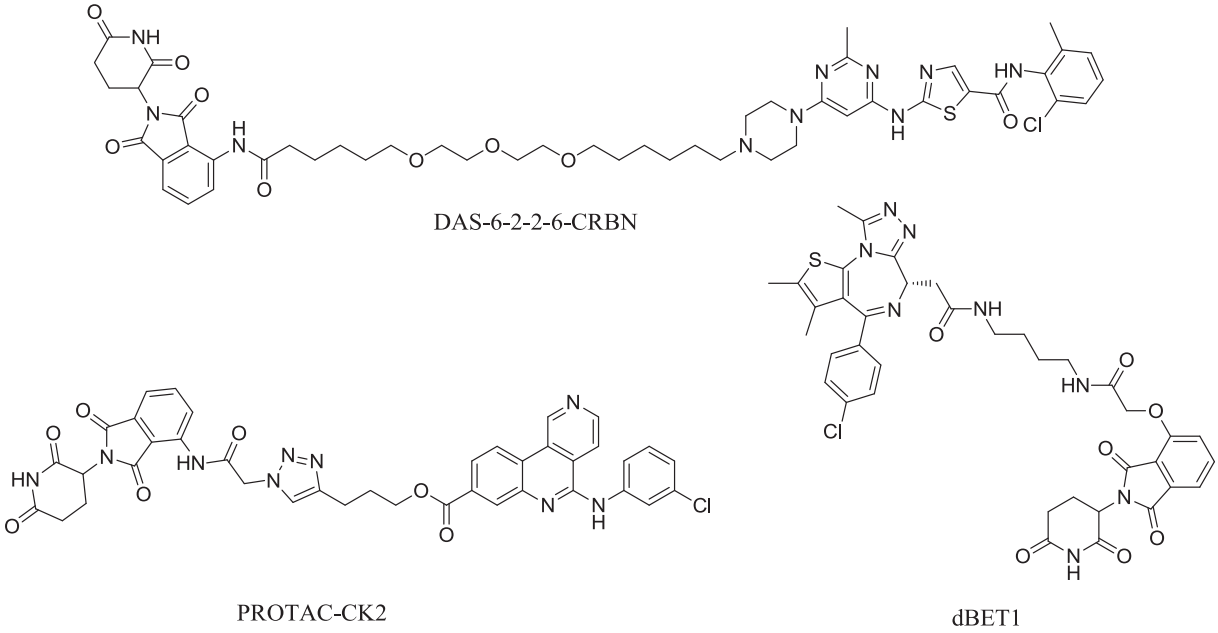

Fig. 2. Several reported PROTACs.

candidate, was firstly developed as a non-ATP-competitive inhibitor of PLK1 [23–25]. Until recent years, it was finally identified as a Ras-mimetic and the direct target of RGS was the Ras-binding domains (RBDs) of Raf protein [26,27]. More importantly, the most common B-Raf mutations, such as the V600E mutation, located in the kinase domain (KD) rather than RBDs. This means that, under most of conditions, the interaction of RGS with B-Raf was not influenced by the mutations. In contrast, most of the kinase inhibitors of B-Raf were susceptible to the mutations resulting in drug resistance [28]. In this study, RGS was selected as the ligand that bound to the POI and several PROTACs targeting B-Raf kinase were synthesized and studied on their anticancer activity and the ability of inducing protein degradation.

2. Results and discussion

2.1. Design and synthesis

It has been reported that RGS (**10**) binds B-Raf RBD in two different orientations, but it occupies the same interface. The intermolecular interaction between RGS and B-Raf is primarily hydrophobic in nature, and the contacts are primarily from the trimethoxy styryl portion and the methoxy benzyl sulfone portion of RGS (Fig. 3). Although the glycine portion of RGS can potentially make a salt link with the guanidino group of R188 amino acid, the portion is exposed in solvent, and the ionic reaction is just observed in one of the binding orientations. Moreover, conjugating of RGS with biotin via the carboxyl in the glycine portion did not influence the interaction between RGS and B-Raf protein, and the biotin-RGS conjugate also could effectively bind to B-Raf [26]. Based on the above findings, the trimethoxy styryl portion and the methoxy benzyl sulfone portion of RGS were strictly retained in the design of the target compounds, and the selection of the linker between RGS moiety and pomalidomide was variable. Due to the protocol that ligands that bind the target anywhere on its surface can be used to make PROTACs that degrade it, this design strategy would be feasible [16,17,19].

Compounds **1**–**4** were synthesized based on the protocol as possible PROTACs (Scheme 1). Pomalidomide (**5**), RGS (**10**) and its intermediate (**9**) were prepared according to a method reported previously [19,23]. **5** was firstly used to react with bromoacetyl chloride and sodium azide subsequently to get **6** and **7**. Then, catalytic hydrogenation of **7** with Pd/C catalyst was carried out to produce **8**. Besides, **11** and **12** were obtained via esterification with corresponding acyl chloride followed by hydrolysis. Finally, compound **1** was synthesized through the reaction of **6** with **9** in methanol solution under refluxing condition in the presence of sodium acetate, and compounds **2**, **3** and **4** were obtained through the esterification of **8** with **10**, **11** or **12**, respectively. All the target compounds **1**–**4** were structurally characterized by elemental analysis, ^{1}H NMR and ^{13}C NMR together with ESI-MS spectrometer.

2.2. The level of B-Raf in different cell lines

As B-Raf, the primary target of RGS moiety, was closely related to the tumorigenesis, its expression level in several cell lines was firstly analyzed before the study of *in vitro* anticancer activity. As shown in Fig. 4, human MCF-7 breast cancer cell line had the highest level of B-Raf in the tested five cell lines, while the expression level of B-Raf in another human breast cancer cell line MDA-MB-231 was apparently lower than that in MCF-7 cells. In human HepG2 hepatoma cells, the expression level of B-Raf was surpassed only by MCF-7 cells. And human normal LO2 liver cells also expressed high level of B-Raf which was in third place in the tested cell lines, and this maybe owe to the rapid regeneration capacity and higher proliferation rate of hepatocytes [29], as well as the irreplaceable role of B-Raf in cell proliferation [30]. It was noteworthy that murine B16 melanoma cells expressed a small

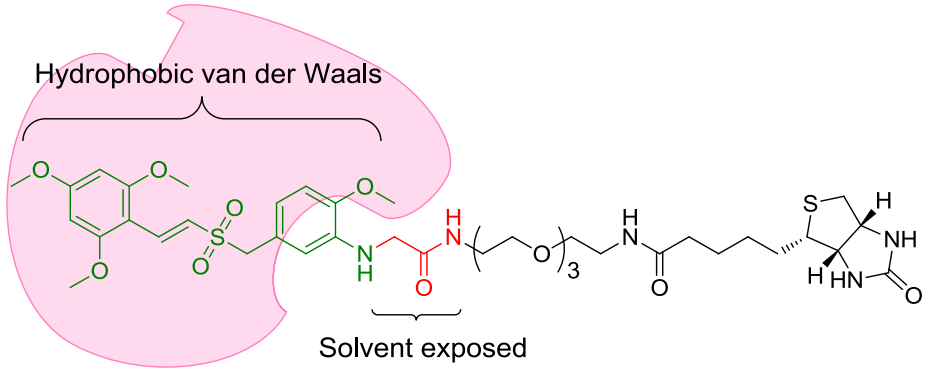

Fig. 3. Structural basis for the design of target compounds.

amount of B-Raf although its mutations were more common in certain clinical and pathologic subsets of melanoma [31].

2.3. In vitro anticancer activity

In vitro cytotoxicities of compounds **1**–**4** against the above five cell lines were measured by MTT assay together with pomalidomide (**5**), RGS (**10**) and its derivative (**9**) as positive references. As shown in Table 1, MCF-7 cancer cells with the highest level of B-Raf were the most sensitive to all the tested compounds targeting B-Raf except for compound **4**. Besides, the cytotoxicities of all tested compounds targeting B-Raf toward human MCF-7 and MDA-MB-231 breast cancer

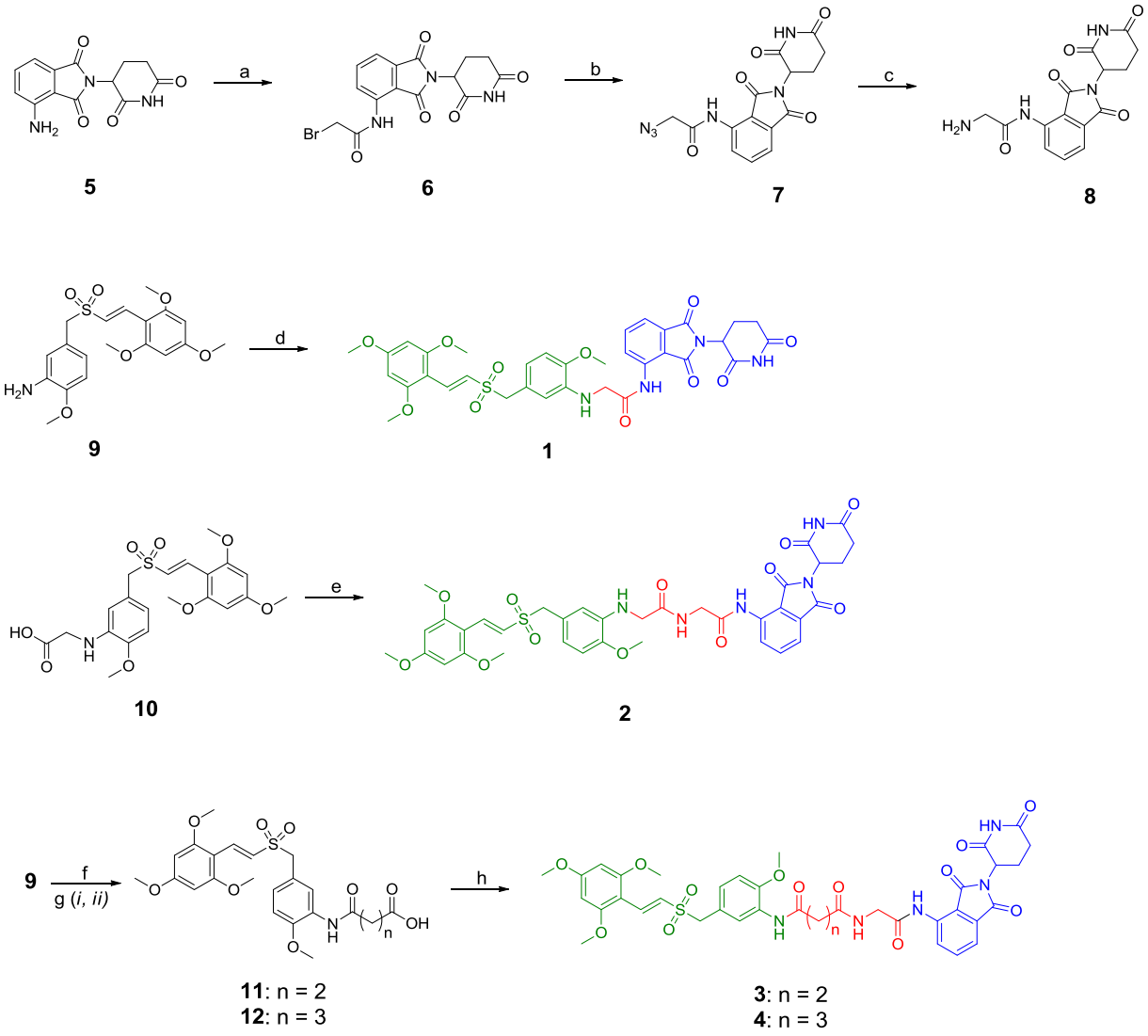

Scheme 1. Synthesis of the target compounds **1**–**4**. (a) bromoacetyl chloride, acetone, reflux for 24 h; (b) NaN_3, acetone, reflux for 24 h; (c) H_2, Pd/C, rt for 6 h; (d) **6**, sodium acetate, methanol, reflux; (e) **8**, TBTU, TAE, DMF, 50 °C for 24 h; (f) ethyl 4-chloro-4-oxobutanoate or ethyl 5-chloro-5-oxopentanoate, DCM, reflux for 24 h; (g) *i:* LiOH·H_2O, ethanol/H_2O, rt, overnight; *ii:* 1 M HCl; (h) **8**, TBTU, TEA, DMF, 50 °C for 24 h.

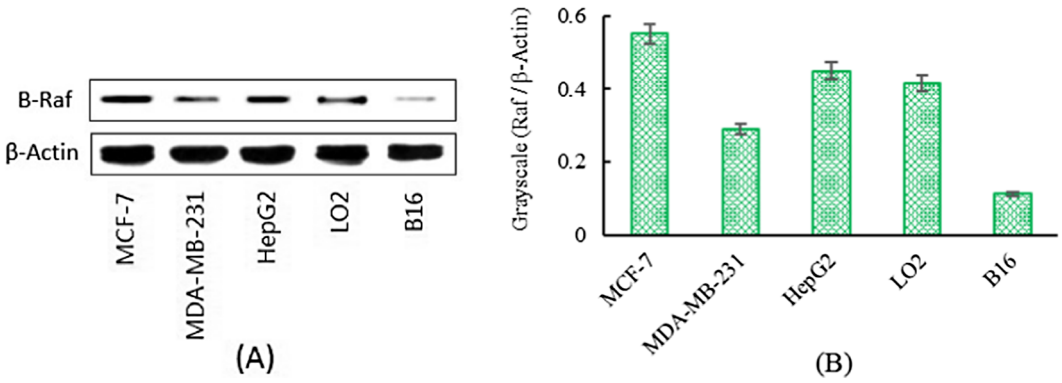

Fig. 4. (A) Western blot and (B) statistic analysis of the expression level of B-Raf in different cell lines based on three independent experiments: human breast cancer cell lines (MCF-7 and MDA-MB-231), human hepatoma cell line (HepG2), murine melanoma cell line (B16) and human normal liver cell line (LO2).

Table 1
Cytotoxicities of tested compounds toward different cell lines.

Compound	IC_{50} (μM)				
	MCF-7	MDA-MB-231	HepG2	LO2	B16
1	12.80 ± 0.98	23.12 ± 2.04	19.25 ± 1.73	> 200	23.67 ± 2.09
2	2.70 ± 0.19	21.21 ± 1.95	18.70 ± 1.65	41.11 ± 3.70	22.68 ± 2.03
3	6.14 ± 0.50	36.96 ± 3.22	11.91 ± 1.02	41.43 ± 3.72	28.53 ± 2.65
4	38.09 ± 3.45	46.23 ± 4.37	14.58 ± 1.31	> 200	29.29 ± 2.74
9	4.17 ± 0.31	21.33 ± 1.96	10.59 ± 0.94	35.57 ± 2.81	14.49 ± 1.28
10	4.46 ± 0.34	25.26 ± 2.28	17.72 ± 1.58	40.27 ± 3.65	12.75 ± 1.01
5	> 200	> 200	> 200	> 200	> 200

IC_{50} is the drug concentration effective in inhibiting 50% of the cell growth measured by the MTT assay after 72 h of drug exposure expressed as the mean value ± standard deviation of three independent experiments.

cells were dependent on the level of B-Raf, and the higher the B-Raf level in the cancer cells, the better the anticancer activities of the compounds. On the other hand, we could find that all tested compounds targeting B-Raf possessed the selectivity between cancer cells and normal cells when compared their cytotoxicities toward human HepG2 hepatoma cells with that toward human normal LO2 liver cells. The selectivity may be due to the fact that ubiquitin-proteasome system (UPS), as the action foundation of PROTAC, was more active in cancer cells [19]. It was worth noting that, although the level of B-Raf in B16 cells was obviously lower than that in MDA-MB-231 cells, there was no significant difference in the cytotoxicities of tested compounds. And this in part because B-Raf mutations were closely related to the occurrence and development of melanoma. All above results implied that both the level of B-Raf and the cell types have great impacts on the *in vitro* anticancer activity of our designed PROTACs. Notably, compound **2** with an IC_{50} value of 2.70 μM toward MCF-7 cells could more effectively kill cancer cells than its mother compounds **9** and **10**, and this presented the potential of compound **2** for the treatment of breast cancer. In addition, pomalidomide (**5**) exhibited almost no cytotoxicity toward all the tested cell lines.

2.4. Degradation of B-Raf

Degradation of B-Raf induced by compound **2** was investigated in MCF-7 cells using pomalidomide (**5**) and compound **9** as references. As shown in Fig. 5, pomalidomide had no influence on the level of B-Raf even at a high concentration of 10 μM, because there was no interaction between pomalidomide and B-Raf. Although compound **9** could directly target B-Raf, it only could disrupt the Ras-Raf interaction and also had little effect on the level of B-Raf. Obviously, the level of B-Raf was dramatically decreased under the treatment of compound **2**, only 28.3% was left at a concentration of 5 μM and 19.0% at 10 μM. The results implied that compound **2** could effectively induce the degradation of B-

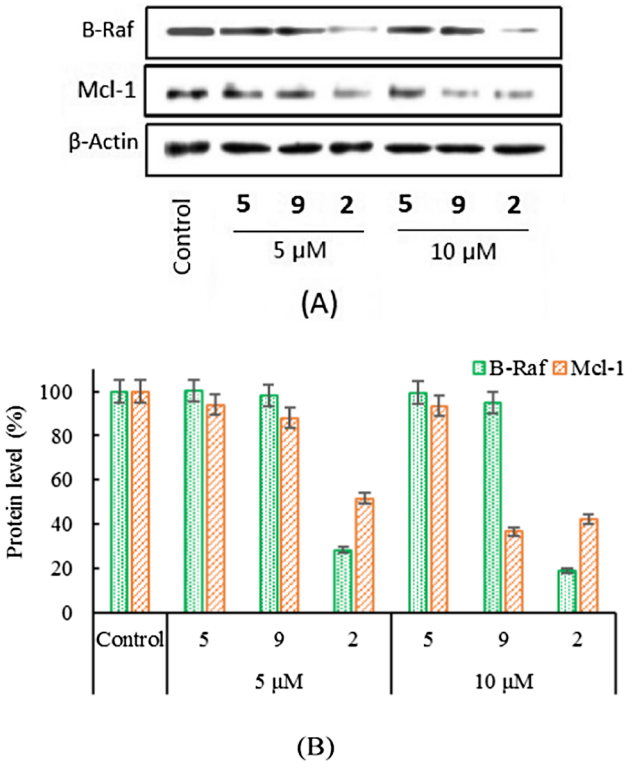

Fig. 5. (A) Western blot image of B-Raf and Mcl-1 in MCF-7 cells after treatment with pomalidomide (**5**), compounds **2** or its mother compound **9** for 24 h at the concentration of 5 μM or 10 μM. (B) Statistic analysis of B-Raf or Mcl-1 level based on three independent experiments.

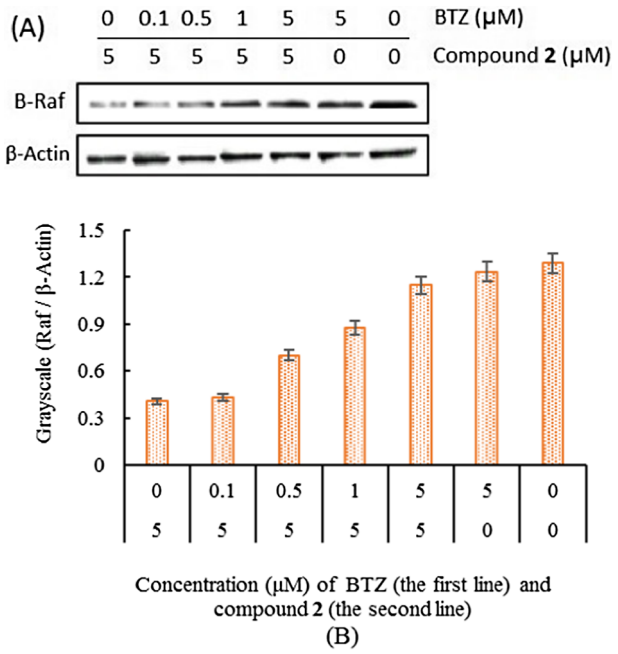

Fig. 6. (A) The levels of B-Raf after pre-treatment with BTZ at different concentrations for 1 h and then treated with compound **2** (5 μM) for 24 h. (B) Statistic analysis of B-Raf level based on three independent experiments.

Raf. It was well known that oncogenic B-Raf can promote the transcriptional upregulation of Mcl-1 [32], as the downstream protein of B-Raf, its level was also detected. Results showed that pomalidomide also could not obviously influence the level of Mcl-1, in contrast, compounds **2** and **9** had great influences on the expression of Mcl-1. Because of the disruption of Ras/Raf pathway, modest downregulation of Mcl-1 was observed under the treatment of compound **9** at a concentration of 5 μM, when its concentration increased to 10 μM, the level of Mcl-1 was remarkably decreased. Whereas, compound **2** could dramatically inhibit the expression of Mcl-1 even at the low concentration of 5 μM. Consequently, compound **2** as an effective PROTAC could induce the degradation of B-Raf and impact the expression of Mcl-1.

2.5. Mechanism of B-Raf degradation

Ubiquitin-proteasome system (UPS) was the action foundation of protein degradation induced by PROTAC, and proteasome as a multicatalytic enzyme could mediate many cellular regulatory signals by degrading ubiquitinated proteins. To confirm the mechanism of the degradation of B-Raf, the first proteasome inhibitor bortezomib (BTZ, originally PS-341) was used for the joint research with compound **2** [33]. As shown in Fig. 6, compound **2** without the pre-treatment of BTZ could degrade B-Raf effectively. After the pre-treatment with BTZ, the degradation of B-Raf was dose-dependently suppressed. Whereas, BTZ had little influence on the level of B-Raf. All above results implied that compound **2** degraded B-Raf through the ubiquitin-proteasome pathway (UPP), and that was completely in conformity with the working principles of PROTAC as expected.

2.6. Apoptosis study

According to the results of cytotoxicity assay, apoptotic analysis of compound **2** against MCF-7 cells were carried out by an Annexin V-FITC/PI assay using its mother compound **9** as reference. As showed in Fig. 7, compounds **2** and **9** owned similar capacity of inducing MCF-7 cells apoptosis at their IC_{50} value respectively for 72 h. When the concentration increased to 20 μM, compound **2** achieved an apoptosis rate of 76.70% (64.00% early apoptosis, 12.70% late apoptosis) after 24 h incubation. While compound **9** only attained an apoptosis rate of 25.80% (25.50% early apoptosis, 0.30% late apoptosis) after 24 h incubation. Apparently, compound **2** was much more effective in promoting apoptosis of MCF-7 cells and the cancer cells seemed to be more sensitive to the PROTAC that worked as a protein degrader.

2.7. Cell cycle analysis

The influence of compound **2** on MCF-7 cell cycle progression was studied by flow cytometry with propidium iodide (PI) staining using compound **9** as a positive control. As shown in Fig. 8, in the control group, 58.27% cells were arrested at G1 phase, 22.31% at S phase, and 19.42% at G2/M phase. Obviously, compounds **2** and **9** arrested cell cycle at the same G2/M phase, and that would attribute to the fact that they had the same target of B-Raf.

3. Conclusions

We have reported the design and synthesis of four pomalidomide hybrids acting as proteolysis targeting chimeras (PROTACs) for the degradation of B-Raf. Human MCF-7 breast cancer cell line was the most sensitive to most of the tested compounds because it had the highest level of B-Raf in the tested cell lines. Among the four PROTACs, compound **2** with an IC_{50} value of 2.70 μM toward MCF-7 cells could more effectively kill cancer cells than its mother compounds. Moreover, it could effectively induce the degradation of B-Raf via the ubiquitin-proteasome pathway, and obviously downregulated the level of Mcl-1, a downstream protein of B-Raf. As a B-Raf degrader, compound **2** was much more potent to promote cancer cell apoptosis and the cancer cells seemed to be more sensitive to the PROTAC. Owing to the facts that B-Raf represents an important target in cancer and the anticancer mechanism of PROTAC was quite different from traditional small molecules, compound **2** possessed the potential for the treatment of breast cancer.

4. Experimental section

4.1. Reagents and instruments

All regents and solvents were obtained from commercial suppliers, and used as received unless otherwise stated. All antibodies used in this study were purchased from Cell Signaling Technology (CST). Mass spectra were measured on an Agilent 6224 TOF LC/MS instrument. Elemental analyses of C, H, and N were carried out using a Vario MICRO CHNOS elemental analyzer (Elementary). ^{1}H NMR and ^{13}C NMR spectra were recorded on a Bruker 400 MHz or 600 MHz spectrometer, using DMSO-d_6 as a solvent. Bio-Rad's iMark microplate absorbance reader was used for MTT assay. Cell cycle and apoptosis experiments were measured by flow cytometry (FAC Scan, Becton Dickenson) and analyzed by Cell Quest software.

4.2. Synthesis and characterization

4.2.1. Synthesis of 2-bromo-N-(2-(2,6-dioxopiperidin-3-yl)-1,3-dioxoisoindolin-4-yl)acetamide (6)

Bromoacetyl chloride (250 μL) was added to a suspension solution of **5** (273.5 mg, 1.0 mmol) in THF, then the mixture was kept stirring under reflux overnight. The mixture was concentrated under reduced pressure, and solids began to deposit after adding diethyl ether. The solid was filtered out and washed with diethyl ether to give compound **6** as a white solid (Yield: 383.0 mg, 97.2%). ESI-MS: $[M+Na]^+$ = 417.98, $[2M+Na]^+$ = 810.98. ^{1}H NMR (ppm, 600 MHz, DMSO-d_6): δ 11.11 (s, 1H), δ 10.27 (s, 1H), δ 8.47 (d, J = 6.0 Hz, 1H), δ 7.88 (t, J = 12.0 Hz, 1H), δ 7.69 (d, J = 6.0 Hz, 1H), δ 5.18 (q, J = 12.0 Hz, 1H), δ 4.34 (s, 2H), δ 2.90 (m, 1H), δ 2.55 (m, 2H), δ 2.08 (m, 1H).

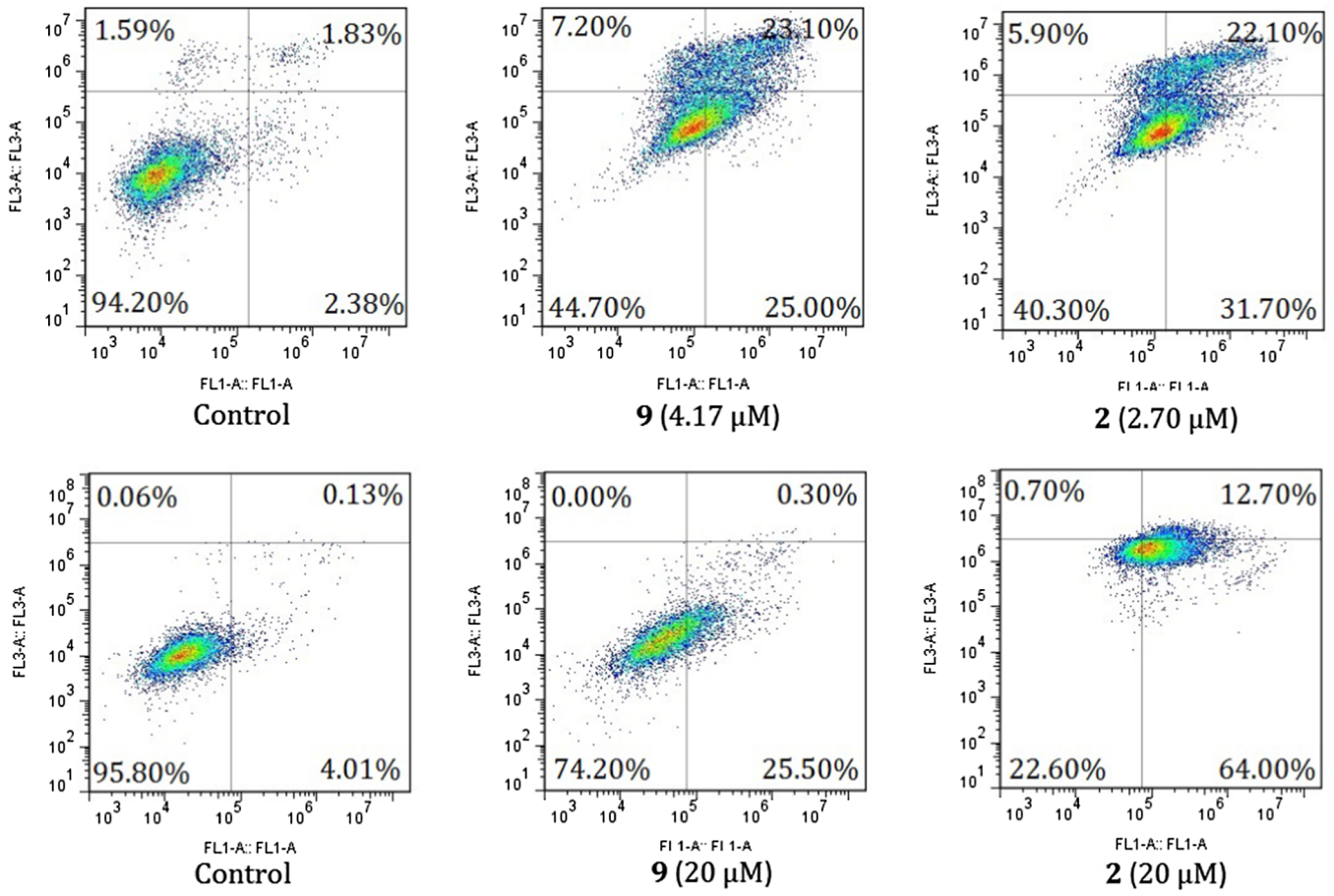

Fig. 7. Flow cytometric analysis of the distribution of MCF-7 cells treated with compounds **2** and **9** at the concentration of IC_{50} values for 72 h or 20 μM for 24 h.

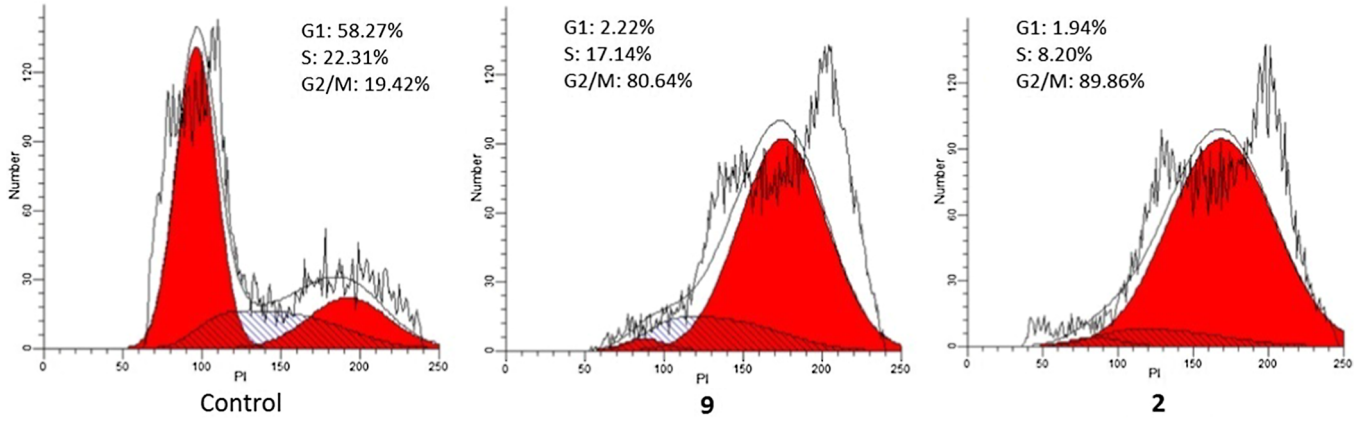

Fig. 8. Cell cycle distributions upon treatment with compounds **2** and **9** at the concentration of 20 μM for 24 h.

4.2.2. Synthesis of 2-azido-N-(2-(2,6-dioxopiperidin-3-yl)-1,3-dioxoisoindolin-4-yl)acetamide (7)

NaN_3 (99.0 mg, 1.52 mmol) was slowly added to a suspension solution of **6** (300.0 mg, 0.76 mmol) in acetone, then the mixture was kept stirring under reflux overnight. The mixture was concentrated under reduced pressure, and solids began to deposit after adding diethyl ether. The solid was filtered out and washed with diethyl ether to give compound **7** as a white solid (Yield: 234.2 mg, 86.5%). ESI-MS: $[M+H]^+$ = 357.09, $[M+Na]^+$ = 379.07. ^1H NMR (ppm, 400 MHz, DMSO-d_6): δ 11.19 (s, 1H), δ 10.17 (s, 1H), δ 8.51 (d, J = 6.0 Hz, 1H), δ 7.88 (t, J = 8.0 Hz, 1H), δ 7.68 (d, J = 8.0 Hz, 1H), δ 5.17 (q, J = 10.0 Hz, 1H), δ 4.55 (s, 2H), δ 2.89 (m, 1H), δ 2.57 (m, 2H), δ 2.02 (m, 1H).

4.2.3. Synthesis of 2-amino-N-(2-(2,6-dioxopiperidin-3-yl)-1,3-dioxoisoindolin-4-yl)acetamide (8)

Pd/C (36.0 mg) was added to a suspension solution of **7** (356.3 mg, 1.0 mmol) in methanol, then the mixture was kept stirring for 6 h under pressurized hydrogen atmosphere at room temperature. Removal of the reaction solvent by evaporation under reduced pressure led to the deposit from the solution. The resulting deposit was dissolved in DMF, then Pd/C was removed by filtration. Next, DMF solution was concentrated under reduced pressure and solids began to deposit after adding diethyl ether. The solid was filtered out and washed with diethyl ether to give compound **8** as an off-white powder (Yield: 210.0 mg, 63.6%). ESI-MS: $[M+H]^+$ = 331.10, $[M+Na]^+$ = 353.08, $[2M+H]^+$ = 661.19, $[2M+Na]^+$ = 683.17. ^1H NMR (ppm, 600 MHz,

DMSO-d_6): δ 11.16 (s, 1H), δ 8.82 (d, J = 6.0 Hz, 1H), δ 7.86 (m, 1H), δ 7.60 (d, J = 6.0 Hz, 1H), δ 5.16 (q, J = 6.0 Hz, 1H), δ 3.34 (s, 2H), δ 2.90 (m, 1H), δ 2.53 (m, 2H), δ 2.07 (m, 1H).

*4.2.4. Synthesis of (E)-4-((2-methoxy-5-(((2,4,6-trimethoxystyryl) sulfonyl)methyl)phenyl)amino)-4-oxobutanoic acid (**11**)*

Ethyl 4-chloro-4-oxobutanoate (1.52 mmol) was added to a suspension solution of **9** (300.0 mg, 0.76 mmol) in DCM, then the mixture was kept stirring under reflux overnight. The organic layer was washed with saturated $NaHCO_3$ solution twice and water once, and dried over sodium sulfate. The filtrate was concentrated under reduced pressure to give the oily intermediate product. Then, the oily product was dissolved in ethanol/H_2O (2:1, v:v) solution and $LiOH{\cdot}H_2O$ was added. The mixture was kept stirring at room temperature overnight. After removal of ethanol, solids began to deposit after adding 0.1 M HCl solution. The solid was filtered out and washed with water to give compound **11** as a white powder (Yield: 256.2 mg, 68.3%). ESI-MS: $[M+Na]^+$ = 516.13, $[2M+Na]^+$ = 1009.27. ^{1}H NMR (ppm, 600 MHz, DMSO-d_6): δ 12.11 (s, 1H), δ 9.14 (d, J = 18.0 Hz, 1H), δ 8.02 (d, J = 24.0 Hz, 1H), δ 7.57 (t, J = 18.0 Hz, 1H), δ 7.10 (m, 3H), δ 6.27 (d, J = 12.0 Hz, 2H), δ 4.33 (d, J = 12.0 Hz, 2H), δ 3.85 (m, 12H), δ 3.02 (d, J = 18.0 Hz, 2H), δ 2.61 (d, J = 18.0 Hz, 2H).

*4.2.5. Synthesis of (E)-5-((2-methoxy-5-(((2,4,6-trimethoxystyryl) sulfonyl)methyl)phenyl)amino)-5-oxopentanoic acid (**12**)*

Same synthetic method of **11** and ethyl 5-chloro-5-oxopentanoate was used to get compound **12** as a white powder (Yield: 241.0 mg, 62.5%). ESI-MS: $[M+Na]^+$ = 530.14, $[2M+Na]^+$ = 1037.29. ^{1}H NMR (ppm, 600 MHz, DMSO-d_6): δ 12.08 (s, 1H), δ 9.08 (s, 1H), δ 7.98 (s, 1H), δ 7.59 (d, J = 12.0 Hz, 1H), δ 7.12 (d, J = 18.0 Hz, 1H), δ 7.04 (m, 2H), δ 6.29 (s, 2H), δ 4.35 (s, 2H), δ 3.85 (m, 12H), δ 2.40 (t, J = 6.0 Hz, 2H), δ 2.26 (t, J = 6.0 Hz, 2H), δ 1.77 (m, 2H).

*4.2.6. Synthesis of (E)-N-(2-(2,6-dioxopiperidin-3-yl)-1,3-dioxoisoindolin-4-yl)-2-((2-methoxy-5-(((2,4,6-trimethoxystyryl)sulfonyl)methyl)phenyl) amino)acetamide (**1**)*

9 (196.7 mg, 0.5 mmol) was added to a solution of **6** (300.0 mg, 0.76 mmol) and sodium acetate (62.5 mg, 0.76 mmol) in methanol and the reaction mixture was kept stirring under reflux. After the reaction was complete, column chromatography (DCM:methanol = 1:1, v:v) gave compound **1** as a white solid (Yield: 162.0 mg, 45.9%). ESI-MS: $[M+Na]^+$ = 729.18,$[2M+Na]^+$ = 1435.37. Anal. Calcd (%) for $C_{34}H_{34}N_4O_{11}S$: C 57.78, H 4.85, N 7.93. Found: C 57.91, H 4.76, N 7.88. ^{1}H NMR (ppm, 600 MHz, DMSO-d_6): δ 11.12 (s, 1H), δ 10.45 (s, 1H), δ 8.73 (d, J = 12.0 Hz, 1H), δ 7.84 (t, J = 6.0 Hz, 1H), δ 7.59 (d, J = 6.0 Hz, 1H), δ 7.51 (d, J = 18.0 Hz, 1H), δ 7.07 (d, J = 12.0 Hz, 1H), δ 6.88 (d, J = 12.0 Hz, 1H), δ 6.67 (d, J = 6.0 Hz, 1H), δ 6.51 (s, 1H), δ 6.25 (s, 2H), δ 5.89 (s, 1H), δ 5.08 (q, J = 6.0 Hz, 1H), δ 4.26 (s, 2H), δ 3.83 (t, J = 6.0 Hz, 14H), δ 2.83 (m, 1H), δ 2.55 (m, 2H), δ 2.00 (m, 1H). ^{13}C NMR (ppm, 150 MHz, DMSO-d_6): δ 173.18, 171.42, 170.23, 168.35, 167.14, 163.98, 161.32, 147.59, 137.63, 136.80, 136.70, 133.20, 131.74, 125.09, 124.03, 121.96, 121.13, 118.61, 116.41, 113.52, 110.63, 102.97, 91.34, 60.61, 56.48, 56.21, 56.03, 49.33, 49.19, 31.34, 22.39.

General synthetic procedure of compounds **2–4**. To a solution of **10**, **11** or **12** (0.33 mmol) in DMF (7.0 mL), TBTU (106.0 mg, 0.33 mmol) and excess TEA were added. The resulting solution was stirred at room temperature for 15 min, then **8** (100.0 mg, 0.30 mmol) was added. After the above mixture was kept under stirring at 50 °C for 24 h, column chromatography (DCM:methanol = 1:1, v:v) gave compounds **2–4** as white solids.

*4.2.7. (E)-N-(2-(2,6-dioxopiperidin-3-yl)-1,3-dioxoisoindolin-4-yl)-2-(2-((2-methoxy-5-(((2,4,6-trimethoxystyryl)sulfonyl)methyl)phenyl)amino) acetamido)acetamide (**2**)*

Yield: 106.0 mg, 46.5%. ESI-MS: $[M+Na]^+$ = 786.19. Anal. Calcd (%) for $C_{36}H_{37}N_5O_{12}S$: C 56.61, H 4.88, N 9.17. Found: C 56.48, H 4.81, N 9.23. ^{1}H NMR (ppm, 600 MHz, DMSO-d_6): δ 11.15 (s, 1H), δ 9.94 (s, 1H), δ 8.69 (t, J = 6.0 Hz, 1H), δ 8.57 (d, J = 6.0 Hz, 1H), δ 7.84 (t, J = 6.0 Hz, 1H), δ 7.62 (d, J = 6.0 Hz, 1H), δ 7.56 (d, J = 12.0 Hz, 1H), δ 7.08 (d, J = 18.0 Hz, 1H), δ 6.82 (d, J = 12.0 Hz, 1H), δ 6.61 (d, J = 6.0 Hz, 1H), δ 6.48 (s, 1H), δ 6.27 (s, 2H), δ 5.35 (s, 1H), δ 5.12 (q, J = 6.0 Hz, 1H), δ 4.26 (s, 2H), δ 3.98 (d, J = 6.0 Hz, 2H), δ 3.85 (m, 14H), δ 2.88 (m, 1H), δ 2.53 (m, 2H), δ 2.07 (m, 1H). ^{13}C NMR (ppm, 150 MHz, DMSO-d_6): δ 173.19, 171.61, 170.23, 169.26, 168.55, 167.13, 164.04, 161.35, 147.06, 137.64, 136.68, 136.54, 133.10, 131.79, 125.56, 124.03, 121.79, 120.04, 118.88, 117.60, 117.00, 112.76, 109.91, 103.00, 91.38, 60.83, 56.53, 56.50, 56.07, 55.90, 49.44, 46.96, 44.00, 31.41, 22.33.

*4.2.8. (E)-N^1-(2-((2-(2,6-dioxopiperidin-3-yl)-1,3-dioxoisoindolin-4-yl) amino)-2-oxoethyl)-N^4-(2-methoxy-5-(((2,4,6-trimethoxystyryl)sulfonyl) methyl)phenyl)succinamide (**3**)*

Yield: 101.0 mg, 42.0%. ESI-MS: $[M+Na]^+$ = 828.21. Anal. Calcd (%) for $C_{38}H_{39}N_5O_{13}S$: C 56.64, H 4.88, N 8.69. Found: C 56.51, H 4.93, N 8.74. ^{1}H NMR (ppm, 600 MHz, DMSO-d_6): δ 11.16 (s, 1H), δ 10.00 (s, 1H), δ 9.15 (s, 1H), δ 8.77 (s, 1H), δ 8.62 (d, J = 6.0 Hz, 1H), δ 8.03 (s, 1H), δ 7.85 (t, J = 6.0 Hz, 1H), δ 7.62 (t, J = 6.0 Hz, 1H), δ 7.58 (s, 1H), δ 7.13 (d, J = 18.0 Hz, 1H), δ 7.00 (m, 2H), δ 6.29 (s, 2H), δ 5.16 (q, J = 6.0 Hz, 1H), δ 4.33 (s, 2H), δ 3.85 (m, 14H), δ 2.88 (m, 1H), δ 2.57 (m, 6H), δ 2.05 (m, 1H). ^{13}C NMR (ppm, 150 MHz, DMSO-d_6): δ 173.22, 173.20, 170.84, 170.24, 169.59, 168.65, 167.12, 164.09, 161.41, 149.65, 136.95, 136.61, 133.37, 131.77, 127.74, 127.32, 125.22, 124.47, 123.99, 121.06, 118.83, 116.77, 111.18, 103.03, 91.39, 60.34, 56.52, 56.20, 56.08, 49.43, 44.03, 31.74, 31.72, 30.68, 22.37.

*4.2.9. (E)-N^1-(2-((2-(2,6-dioxopiperidin-3-yl)-1,3-dioxoisoindolin-4-yl) amino)-2-oxoethyl)-N^5-(2-methoxy-5-(((2,4,6-trimethoxystyryl)sulfonyl) methyl)phenyl)glutaramide (**4**)*

Yield: 145.0 mg, 59.0%. ESI-MS: $[M+Na]^+$ = 842.23. Anal. Calcd (%) for $C_{39}H_{41}N_5O_{13}S$: C 57.14, H 5.04, N 8.54. Found: C 57.28, H 4.97, N 8.63. ^{1}H NMR (ppm, 600 MHz, DMSO-d_6): δ 11.16 (s, 1H), δ 10.01 (s, 1H), δ 9.08 (s, 1H), δ 8.70 (t, J = 6.0 Hz, 1H), δ 8.23 (d, J = 12.0 Hz, 1H), δ 8.02 (s, 1H), δ 7.86 (t, J = 6.0 Hz, 1H), δ 7.62 (t, J = 6.0 Hz, 1H), δ 7.59 (s, 1H), δ 7.13 (d, J = 12.0 Hz, 1H), δ 7.04 (m, 2H), δ 6.29 (s, 2H), δ 5.15 (q, J = 6.0 Hz, 1H), δ 4.36 (s, 2H), δ 3.85 (m, 14H), δ 2.86 (m, 1H), δ 2.59 (m, 2H), δ 2.42 (t, J = 6.0 Hz, 2H), δ 2.34 (t, J = 6.0 Hz, 2H), δ 2.05 (m, 1H), δ 1.86 (t, J = 6.0 Hz, 2H). ^{13}C NMR (ppm, 150 MHz, DMSO-d_6): δ 173.62, 173.25, 172.62, 171.40, 170.26, 169.66, 168.70, 167.13, 164.09, 161.46, 161.40, 155.05, 149.93, 136.98, 136.64, 133.36, 131.78, 127.66, 127.50, 125.17, 124.00, 121.05, 118.82, 116.66, 111.23, 103.00, 91.37, 60.27, 59.63, 56.52, 56.20, 56.07, 49.44, 44.04, 35.92, 34.89, 32.75, 31.37, 22.36.

4.3. Cell lines and cell culture

Human breast cancer cell lines (MCF-7 and MDA-MB-231), human hepatoma cell line (HepG2), murine melanoma cell line (B16) and human normal liver cell line (LO2) were purchased from Jiangsu KeyGen BioTECH Co. Ltd. Cells were incubated carefully in RPMI-1640 medium or Dulbecco's Modified Eagle Medium (DMEM) supplemented with 10% fetal bovine serum (FBS), streptomycin (100 μg/mL), and ampicillin sodium (100 μg/mL) in an atmosphere of 5% CO_2 and 95% air at 37 °C.

4.4. Western blotting

After the treatment with the indicated concentration of each sample for 24 h, cells were collected and lysed in lysis buffer (100 mM Tris-Cl, pH 6.8, 4% (m/v) sodium dodecylsulfonate, 20% (v/v) glycerol, 200 mM β-mercaptoethanol, 1 mM phenylmethylsulfonyl fluoride, and 1 g/mL aprotinin). Lysates were centrifuged at 12,000 g for 0.5 h at

4 °C. The concentrations of total proteins were measured using the BCA assay method with Varioskan spectrofluorometer and spectrophotometer (Thermo, Waltham, MA) at 562 nm. Protein (20–100 μg) prepared from the indicated cells was loaded per lane and electrophoresed in 8% or 10% sodium dodecyl sulfate polyacrylamide gel electrophoresis (SDS-PAGE), and then transferred onto polyvinylidene difluoride (PVDF) Immobilon-P membrane (Bio-Rad, USA) using a transblot apparatus (Bio-Rad, USA). The membranes were blocked with 5% (w/v) non-fat milk at 0.5 h at 37 °C, followed by overnight incubation at 4 °C with primary antibodies diluted in PBST. After washing with PBST, the membranes were incubated for 1 h with an IRDye'800 conjugated secondary antibody diluted 1:1000 in PBST, and the labeled proteins were detected with an Odyssey Scanning System (Li-COR., Lincoln, Nebraska, USA).

4.5. Cytotoxicity measurement

The cultured cells with better vitality were transferred to a 96-well plate so that the density of the cells was 5000 per well, and they were incubated overnight. Then, the compounds were dissolved in DMSO and diluted with medium to various concentrations (the final concentration of DMSO was less than 0.4%). After being incubated at 37 °C for 72 h, cells were stained with 3-(4,5-dimethyl-2-thiazolyl)-2,5-diphenyl-2Htetrazolium bromide (MTT, 5 mg/mL) for another 4 h, and then dissolved with 150 μL of DMSO. The UV absorption intensity was detected with an ELISA reader at 490 nm. The IC_{50} values were calculated by SPSS software after three parallel experiments.

4.6. Apoptosis analysis

MCF-7 cells with good activity (1 × 105 cells per plate) were transferred to six-well plates and cultured overnight in 5% CO_2 at 37 °C. The tested compounds were diluted to the specified concentration. After 24 h or 72 h, the cells were digested with trypsin and washed with cold PBS, and collected by centrifugation (2000 rpm, 5 min). After that, cells were resuspended in binding buffer (10 mM HEPES, 140 mM NaCl, 2.5 mM $CaCl_2$, pH 7.4) and incubated with annexin V-FITC (100 ng/mL) and then with propidium iodide (2 μg/mL) for 15 min in the dark at room temperature. At last, the fluorescence was measured using a flow cytometer (FACScan, Becton Dickson, USA).

4.7. Cell cycle measurement

MCF-7 cells with good vitality were transferred into six-well plates, with a density of 10,000 cells per well, and cultured overnight at 37 °C. Then, 20 μM of the tested compounds were incubated with cells for 24 h. All adherent and floating cells were collected and washed twice with PBS. Then, the cells were fixed with 70% EtOH at 4 °C for 24 h. After that, fixed cells were washed with PBS. After being centrifuged, cells were stained with 50 μg/mL propidium iodide solution containing 100 μg/mL RNase at 37 °C for 0.5 h. The samples (at least 10,000 cells) were measured by flow cytometry (FAC Scan, Becton Dickenson) using Cell Quest software and recording propidium iodide (PI) in the FL2 channel.

Acknowledgements

We are grateful to the National Natural Science Foundation of China (Nos. 21571033 and 81503099) and Southeast University "Perfect Young Scholars" Support Program. Fundamental Research Funds for the Central Universities (Projects 2242016K30020 and 2242017K41024) and Priority Academic Program Development of Jiangsu Higher Education Institutions for the construction of fundamental facilities are also appreciated.

Notes

The authors declare no competing financial interest.

Appendix A. Supplementary data

Supplementary data to this article can be found online at https://doi.org/10.1016/j.bioorg.2019.03.035.

References

[1] C. Galustian, M.C. Labarthe, J.B. Bartlett, A.G. Dalgleish, Thalidomide-derived immunomodulatory drugs as therapeutic agents, Expert Opin. Boil. Ther. 4 (2004) 1963–1970.
[2] C. Galustian, B. Meyer, M.C. Labarthe, K. Dredge, D. Klaschka, J. Henry, S. Todryk, R. Chen, G. Muller, D. Stirling, P. Schafer, J.B. Bartlett, A.G. Dalgleish, The anti-cancer agents lenalidomide and pomalidomide inhibit the proliferation and function of T regulatory cells, Cancer Immunol. Immun. 58 (2009) 1033–1045.
[3] H. Quach, D. Ritchie, A.K. Stewart, P. Neeson, S. Harrison, M.J. Smyth, H.M. Prince, Mechanism of action of immunomodulatory drugs (IMiDS) in multiple myeloma, Leukemia 24 (2010) 22–32.
[4] R.J. D'Amato, M.S. Loughnan, E. Flynn, J. Folkman, Thalidomide is an inhibitor of angiogenesis, Proc. Natl. Acad. Sci. USA 91 (1994) 4082–4085.
[5] T. Ito, H. Ando, T. Suzuki, T. Ogura, K. Hotta, Y. Imamura, Y. Yamaguchi, H. Handa, Identification of a primary target of thalidomide teratogenicity, Science 327 (2010) 1345–1350.
[6] E.S. Fischer, K. Böhm, J.R. Lydeard, H. Yang, M.B. Stadler, S. Cavadini, J. Nagel, F. Serluca, V. Acker, G.M. Lingaraju, R.B. Tichkule, M. Schebesta, W.C. Forrester, M. Schirle, U. Hassiepen, J. Ottl, M. Hild, R.E.J. Beckwith, J. Wade Harper, J.L. Jenkins, N.H. Thomä, Structure of the DDB1–CRBN E3 ubiquitin ligase in complex with thalidomide, Nature 512 (2014) 49–53.
[7] M.Q. Lacy, A.R. McCurdy, Pomalidomide, Blood 122 (2013) 2305–2309.
[8] A.A. Chanan-Khan, A. Swaika, A. Paulus, S.K. Kumar, J.R. Mikhael, S.V. Rajkumar, A. Dispenzieri, M.Q. Lacy, Pomalidomide: the new immunomodulatory agent for the treatment of multiple myeloma, Blood Cancer J. 3 (2013) e143.
[9] A. Lopez-Girona, D. Mendy, T. Ito, K. Miller, A.K. Gandhi, J. Kang, S. Karasawa, G. Carmel, P. Jackson, M. Abbasian, A. Mahmoudi, B. Cathers, E. Rychak, S. Gaidarova, R. Chen, P.H. Schafer, H. Handa, T.O. Daniel, J.F. Evans, R. Chopra, Cereblon is a direct protein target for immunomodulatory and antiproliferative activities of lenalidomide and pomalidomide, Leukemia 26 (2012) 2445–2445.
[10] G. Petzold, E.S. Fischer, N.H. Thomä, Structural basis of lenalidomide-induced CK1α degradation by the CRL4CRBN ubiquitin ligase, Nature 532 (2016) 127–130.
[11] J. Krönke, N.D. Udeshi, A. Narla, P. Grauman, S.N. Hurst, M. McConkey, T. Svinkina, D. Heckl, E. Comer, X. Li, C. Ciarlo, E. Hartman, N. Munshi, M. Schenone, S.L. Schreiber, S.A. Carr, B.L. Ebert, Lenalidomide causes selective degradation of IKZF1 and IKZF3 in multiple myeloma cells, Science 343 (2014) 301–305.
[12] K.M. Sakamoto, K.B. Kim, A. Kumagai, F. Mercurio, C.M. Crews, R.J. Deshaies, Protacs: Chimeric molecules that target proteins to the Skp1-Cullin-F box complex for ubiquitination and degradation, Proc. Natl. Acad. Sci. USA 98 (2001) 8554–8559.
[13] I. Churcher, Protac-induced protein degradation in drug discovery: breaking the rules or just making new ones? J. Med. Chem. 61 (2018) 444–452.
[14] M. Toure, C.M. Crews, Small-molecule PROTACS: new approaches to protein degradation, Angew. Chem. Int. Edit. 55 (2016) 1966–1973.
[15] P.M. Cromm, C.M. Crews, Targeted protein degradation: from chemical biology to drug discovery, Cell Chem. Biol. 24 (2017) 1181–1190.
[16] K. Raina, C.M. Crews, Targeted protein knockdown using small molecule degraders, Curr. Opin. Chem. Biol. 39 (2017) 46–53.
[17] A.C. Lai, M. Toure, D. Hellerschmied, J. Salami, S. Jaime-Figueroa, E. Ko, J. Hines, C.M. Crews, Modular PROTAC design for the degradation of oncogenic BCR-ABL, Angew. Chem. Int. Edit. 55 (2016) 807–810.
[18] G.E. Winter, D.L. Buckley, J. Paulk, J.M. Roberts, A. Souza, S. Dhe-Paganon, J.E. Bradner, Phthalimide conjugation as a strategy for in vivo target protein degradation, Science 348 (2015) 1376–1381.
[19] H. Chen, F. Chen, N. Liu, X. Wang, S. Gou, Chemically induced degradation of CK2 by proteolysis targeting chimeras based on a ubiquitin-proteasome pathway, Bioorg. Chem. 81 (2018) 536–544.
[20] H. Davies, G.R. Bignell, C. Cox, P. Stephens, S. Edkins, S. Clegg, J. Teague, H. Woffendin, M.J. Garnett, W. Bottomley, N. Davis, E. Dicks, R. Ewing, Y. Floyd, K. Gray, S. Hall, R. Hawes, J. Hughes, V. Kosmidou, A. Menzies, C. Mould, A. Parker, C. Stevens, S. Watt, S. Hooper, R. Wilson, H. Jayatilake, B.A. Gusterson, C. Cooper, J. Shipley, D. Hargrave, K. Pritchard-Jones, N. Maitland, G. Chenevix-Trench, G.J. Riggins, D.D. Bigner, G. Palmieri, A. Cossu, A. Flanagan, A. Nicholson, J.W.C. Ho, S.Y. Leung, S.T. Yuen, B.L. Weber, H.F. Seigler, T.L. Darrow, H. Paterson, R. Marais, C.J. Marshall, R. Wooster, M.R. Stratton, P. Andrew, Futreal, mutations of the BRAF gene in human cancer, Nature 417 (2002) 949–954.
[21] K.T. Flaherty, G. Mcarthur, BRAF, a target in melanoma: implications for solid tumor drug development, Cancer 116 (2010) 4902–4913.
[22] T. Rajakulendran, M. Sahmi, M. Lefrançois, F. Sicheri, M. Therrien, A dimerization-dependent mechanism drives RAF catalytic activation, Nature 461 (2009) 542–545.
[23] M.V.R. Reddy, P. Venkatapuram, M.R. Mallireddigari, V.R. Pallela, S.C. Cosenza,

K.A. Robell, B. Akula, B.S. Hoffman, E. Premkumar Reddy, Discovery of a clinical stage multi-kinase inhibitor sodium (E)-2-{2-Methoxy-5-[(2',4',6'-trimethoxystyrylsulfonyl) methyl] phenylamino}acetate (ON 01910.Na): synthesis, structure-activity relationship, and biological activity, J. Med. Chem. 54 (2011) 6254–6276.

[24] K. Gumireddy, M.V. Ramana Reddy, S.C. Cosenza, R. Boomi Nathan, S.J. Baker, N. Papathi, J. Jiang, J. Holland, E. Premkumar Reddy, ON01910, a non-ATP-competitive small molecule inhibitor of Plk1, is a potent anticancer agent, Cancer Cell 7 (2005) 275–286.

[25] D.W. Bowles, J.R. Diamond, E.T. Lam, C.D. Weekes, D.P. Astling, R.T. Anderson, S. Leong, L. Gore, M. Varella-Garcia, B.W. Vogler, S.B. Keysar, E. Freas, D.L. Aisner, C. Ren, A.C. Tan, F. Wilhelm, M. Maniar, S. Gail Eckhardt, W.A. Messersmith, A. Jimeno, Phase I study of oral rigosertib (ON 01910.Na), a dual inhibitor of the PI3K and Plk1 pathways, in adult patients with advanced solid malignancies, Clin. Cancer Res. 20 (2014) 1656–1665.

[26] S.K. Athuluri-Divakar, R. Vasquez-Del Carpio, K. Dutta, S.J. Baker, S.C. Cosenza, I. Basu, Y.K. Gupta, M.V. Ramana Reddy, L. Ueno, J.R. Hart, P.K. Vogt, D. Mulholland, C. Guha, A.K. Aggarwal, E. Premkumar Reddy, A small molecule RAS-mimetic disrupts RAS association with effector proteins to block signaling, Cell 165 (2016) 643–655.

[27] E.P. Reddy, S.K. Divakar, R. Vasquez-Del Carpio, K. Dutta, S.J. Baker, R. Reddy, A.K. Aggarwal, Rigosertib blocks RAS signaling by acting as a small molecule RAS mimetic that binds to the RAS-Binding domains of RAS effector proteins, Blood 124 (2014) 5616–5616.

[28] J. Villanueva, A. Vultur, J.T. Lee, R. Somasundaram, M. Fukunaga-Kalabis, A.K. Cipolla, B. Wubbenhorst, X. Xu, P.A. Gimotty, D. Kee, A.E. Santiago-Walker, R. Letrero, K. D'Andrea, A. Pushparajan, J.E. Hayden, K.D. Brown, S. Laquerre, G.A. McArthur, J.A. Sosman, K.L. Nathanson, M. Herlyn, Acquired resistance to BRAF inhibitors mediated by a RAF kinase switch in melanoma can be overcome by cotargeting MEK and IGF-1R/PI3K, Cancer Cell 18 (2010) 683–695.

[29] S. Lee, RAF-targeted therapy for hepatocellular carcinoma in the regenerating liver, J. Surg. Oncol. 107 (2013) 393–401.

[30] D.N. Chadee, J.M. Kyriakis, A novel role for mixed lineage kinase 3 (MLK3) in B-Raf activation and cell proliferation, Cell Cycle 3 (2004) 1227–1229.

[31] K.T. Flaherty, M.B. Grant McArthur, BRAF a target in melanoma, Cancer 116 (2010) 4902–4913.

[32] T.M. Becker, S.C. Boyd, B. Mijatov, K. Gowrishankar, S. Snoyman, G.M. Pupo, R.A. Scolyer, G.J. Mann, R.F. Kefford, X.D. Zhang, H. Rizos, Mutant B-RAF-Mcl-1 survival signaling depends on the STAT3 transcription factor, Oncogene 33 (2014) 1158–1166.

[33] J. Adams, M. Kauffman, Development of the proteasome inhibitor Velcade™(Bortezomib), Cancer Invest. 22 (2004) 304–311.